THE EFFECT OF CONFINEMENT IN DOUBLE PHOTOEMISSION

N. Fominykh, J. Berakdar
Max-Planck-Institut für Mikrostrukturphysik
Weinberg 2, D-06120 Halle (Saale), Germany

Abstract The aim of this work is to highlight the role of confinement and electron-electron interaction in the double photoemission spectra. We probe simple models, bridging the 'atomic' case of the process with its 'surface' counterpart via the prototypes of a quantum dot and a thin film. The manifestation of two aspects - localization of the electronic states in confined systems and the role of screening in extended systems - is illustrated in the DPE angular distributions.

Keywords: Quantum-size effects, photoemission, double photoemission, electronic correlation, confinement, localisation.

1. INTRODUCTION

In one-photon two-electron photoemission (DPE) experiments from solids and surfaces one resolves simultaneously the energies and emission angles of two photoelectrons for well defined properties of the photon field and the sample under study [1]. As the escape depth of low-energy electrons is of the order of a few atomic layers the low-energy photoelectrons are produced in the surface region. The theoretical analysis of the DPE shows that the two-electron coincident signal is an evident signature of inter-electronic interactions [2,3]. In extended systems electronic correlation is intimately related to localization of electronic states. Thus, the question arises as to what extent the confinement (and/or dimensionality) of the scattering volume may effect the DPE spectra. Dimensionality could be also meant in context with the dimensionality of the Coulomb interaction, as is discussed e.g. in [4]. Here the electron-electron interaction will be assumed three-dimensional, which is the most general and physically relevant choice.

In the present work simple models will be probed, trying to bridge 'atomic' version of the process with its 'surface' counterpart via the

Many-Particle Spectroscopy of Atoms, Molecules, Clusters, and Surfaces, edited by Berakdar and Kirschner, Kluwer Academic/Plenum Publishers, New York 2001

prototypes of a quantum dot and a thin film. In the case of a film electrons have discrete energy levels in one direction and are free to move in the other two. In the case of a quantum dot the electrons are confined in all three directions and have only discrete bound states. For these systems we write down DPE matrix elements and cross sections (Sec.2). The size of a quantum dot can vary from tens to hundreds angstroms, giving a broad range of distances over which it's bound states can spread. Thus our first aim is to probe the size-effect in DPE angular distributions from a dot (Sec.3). Our second aim is the inclusion of the interaction of the two photoelectrons with all the other surrounding electrons. This may be approximately done within the static-screening concept. The role of screening in DPE spectra from a thin film is discussed in Sec.4.

2. FORMALISM AND APPROXIMATIONS

We consider a process in which an incident photon (energy $\hbar\omega$) knocks two electrons out of a system S, the properties of which will be specified further. The subsequent detection of both outgoing electrons in coincidence allows the simultaneous determination of their wave vectors $\mathbf{k}_1$ and $\mathbf{k}_2$. In the sudden approximation the photon field affects only the degrees of freedom of the two electrons, which will be termed 'active', in contrast to the remaining 'passive' ground state electrons of S. The latter do not participate in the dipole transition explicitly, but can alter the strength and range of the interaction between two active electrons. The transition matrix element in the dipole velocity form is

$$T = \langle \Psi_{12} | \hat{\epsilon} \cdot (\nabla_1 + \nabla_2) | \Phi_{12} \rangle , \tag{1}$$

for the transition between two-electron initial $|\Phi_{12}\rangle$ and final $\langle \Psi_{12}|$ states, $\hat{\epsilon}$ being a photon polarization vector. We employ a simple initial state constructed as an antisymmetrized product of single-particle states of the system S (spin-orbit interaction is neglected and the spin part is factored out):

$$\Phi_{12}(\mathbf{r}_1, \mathbf{r}_2) = \Phi_1(\mathbf{r}_1)\Phi_2(\mathbf{r}_2) \pm \Phi_2(\mathbf{r}_1)\Phi_1(\mathbf{r}_2). \tag{2}$$

We assume that the system S remains neutral upon photoionization, which is reasonable for the system with the large number of electrons. The final state is generated by back-propagating the asymptotic plane-wave state $|\mathbf{k}_1, \mathbf{k}_2\rangle$ via the total Green operator G_{12}

$$\Psi_{12}(\mathbf{r}_1, \mathbf{r}_2) = G_{12} |\mathbf{k}_1, \mathbf{k}_2\rangle \tag{3}$$

The Green operator G_{12} is given by the integral equation

$$G_{12} = G_0 + G_0 (V_1 + V_2 + V_{12}) G_{12}. \tag{4}$$

Here, G_0 is the free Green operator, V_1 and V_2 couple electrons to the system S, and V_{12} is assumed to be either bare or screened Coulomb interaction, depending on the purposes and on the system at hand. The potential in Eq.(4) contains only two-body interactions, which leads to the reduction of the total Green's operator in terms of lower-order operators:

$$G_{12} = \mathcal{G}_0^{-2}\mathcal{G}_1\mathcal{G}_2\mathcal{G}_{12}, \tag{5}$$

where the operators $\mathcal{G}_j$ are given by $\mathcal{G}_j = G_0 + G_0 V_j \mathcal{G}_j$ $j = \{1, 2, 12\}$.

In the following we neglect the interaction of the final-state electrons with the system S, In the case of bare Coulomb interaction we also approximate the Green's function G_{12} by that of the relative motion, depending on the relative coordinate $\mathbf{r} = \mathbf{r}_1 - \mathbf{r}_2$. This approximation corresponds to the calculation of the two-electron state (3) in the free space, still keeping the interaction with the system S in the initial state Eq.(2).

To deduce the optical double transition amplitude we transform to the Jacobi coordinates $\mathbf{K}^+ = \mathbf{k}_1 + \mathbf{k}_2$ and $\mathbf{K}^- = (\mathbf{k}_2 - \mathbf{k}_1)/2$ to arrive at

$$\begin{aligned}
T \;\propto\; & \int \langle \mathbf{K}^+\mathbf{K}^- | G_{12}(\hat{\epsilon}\cdot\mathbf{P}^+) | \mathbf{P}^-\mathbf{P}^+ \rangle \langle \mathbf{P}^-\mathbf{P}^+ | \mathbf{p}_1\mathbf{p}_2 \rangle \times \\
\times\; & \langle \mathbf{p}_1, \mathbf{p}_2 | \Phi_{12} \rangle \, d^3\mathbf{P}^+ \mathrm{d}^3\mathbf{P}^- \mathrm{d}^3\mathbf{p}_1 \mathrm{d}^3\mathbf{p}_2 = \\
= \; & \int (\hat{\epsilon}\cdot\mathbf{P}^+)\delta(\mathbf{P}^+ - \mathbf{K}^+) \langle \mathbf{K}^- | \mathrm{G}_{12} | \mathbf{P}^- \rangle \langle \mathbf{P}^-\mathbf{P}^+ | \mathbf{p}_1\mathbf{p}_2 \rangle \times \\
\times\; & \langle \mathbf{p}_1, \mathbf{p}_2 | \Phi_{12} \rangle \, d^3\mathbf{P}^+ \mathrm{d}^3\mathbf{P}^- \mathrm{d}^3\mathbf{p}_1 \mathrm{d}^3\mathbf{p}_2 = \\
= \; & \int (\hat{\epsilon}\cdot\mathbf{P}^+)\delta(\mathbf{p}_3 + \mathbf{p}_4 - \mathbf{k}_1 - \mathbf{k}_2) \left\langle \frac{1}{2}(\mathbf{k}_2 - \mathbf{k}_1) \middle| \mathrm{G}_{12} \middle| \frac{1}{2}(\mathbf{p}_4 - \mathbf{p}_3) \right\rangle \times \\
\times\; & \langle \mathbf{p}_3, \mathbf{p}_4 | \Phi_{12} \rangle \, d^3\mathbf{p}_3 \mathrm{d}^3\mathbf{p}_4 = \\
= \; & (\hat{\epsilon}\cdot\mathbf{K}^+) \int \mathrm{d}^3\mathbf{p}_3 \left\langle \frac{1}{2}(\mathbf{k}_2 - \mathbf{k}_1) \middle| \mathrm{G}_{12} \middle| \frac{1}{2}(\mathbf{k}_1 + \mathbf{k}_2) - \mathbf{p}_3 \right\rangle \times \\
\times\; & \langle \mathbf{p}_3, \mathbf{k}_1 + \mathbf{k}_2 - \mathbf{p}_3 | \Phi_{12} \rangle \,.
\end{aligned} \tag{6}$$

This expression exhibits the DPE selection rule $\hat{\epsilon}(\mathbf{k}_1 + \mathbf{k}_2) \neq 0$, which implies that the photon acts on the center of mass of two electrons. The matrix element of the Green's function embodies the dynamical correlation effects as described by the motion of the relative coordinate in the Coulomb field [5]. It is given by the Fourier transform of the Coulomb continuum wave function [5]. The Fourier transform of the initial state $\langle \mathbf{p}_3, \mathbf{k}_1 + \mathbf{k}_2 - \mathbf{p}_3 | \Phi_{12} \rangle$ characterises the overlap of the single-electron orbitals in the momentum space and is strongly dependent on the spatial extention of the system and on the particular final state total momen-

tum $\mathbf{k}_1 + \mathbf{k}_2$. In the following our intention is to use simple confining potentials for the initial state wave functions, which would merely reflect the main physical aspect - the degree of the localization of states.

3. THREE-DIMENSIONAL CONFINEMENT

The parabolic well is a usual shape to describe a potential of a quantum dot. The simplest form of the potential is given by the spherically symmetric oscillator; the modifications allow for different frequencies an effective masses in x, y, z-directions [6]. There is a temptation to take the wave functions of the exact infinite well problem for the construction of the initial state, but such a dot would have no ionization continuum. So, we solve eigenvalue-eigenfunction problem for the finite well numerically. We will assume that the lateral extension of the potential is larger (or equal) than that in z-direction, and the confinement energies in x and y directions are assumed equal for simplicity:

$$V(x,y,z) = \frac{1}{2} m^*_{||} \omega^2_{||} \left(x^2 + y^2\right) + \frac{1}{2} m^*_{\perp} \omega^2_{\perp} z^2, \qquad \omega_{||} < \omega_{\perp} \tag{7}$$

The single-particle density of states is given by the delta-functions $\rho(E) = \sum_i \delta(E - E_i)$, where i counts all the (degenerated) levels.

The 6-fold DPE differential cross section is

$$\frac{d\sigma}{dE_1 dE_2 d\Omega_1 d\Omega_2} \propto \int |T|^2 \, \delta(E_i - E_f) \rho(E_a) \rho(E_b) dE_a dE_b \tag{8}$$

where E_a and E_b are the energies of the electrons in the initially bound states and E_i and E_f are the the initial and final state energies, respectively, i.e.

$$E_i = E_a + E_b + \hbar\omega, \qquad E_f = \frac{k_1^2 + k_2^2}{2}. \tag{9}$$

The DPE angular correlation discussed in this section is an angular distribution of one of the electrons over two angles θ and φ, while the emission angles of the second electron are fixed and the direction of polarization vector $\hat{\epsilon}$ is well defined. For space limitations we present here only two typical examples. We consider a spherical oscillator potential of a constant depth (V_0=300 meV) and a radius ranging from 7 to 400 Å. Suppose that only the lowest level is occupied. This means that the initial state is a singlet and the total final state energy $E_1 + E_2$ is fixed by the photon energy. Fig.1 shows the case of $E_1 = 1\ eV$, $E_2 = 19\ eV$, $\theta_1 = 0$, $\phi_1 = 0$, the vector $\hat{\epsilon}$ is perpendicular to the emission direction of the first electron. The angle $\phi_2 = 0$, and the DPE intensities are plotted as functions of θ_2. The minimum at $\theta_2 = 0$ arrises due to the DPE selection rule exposed above: The two electrons can not be emitted with

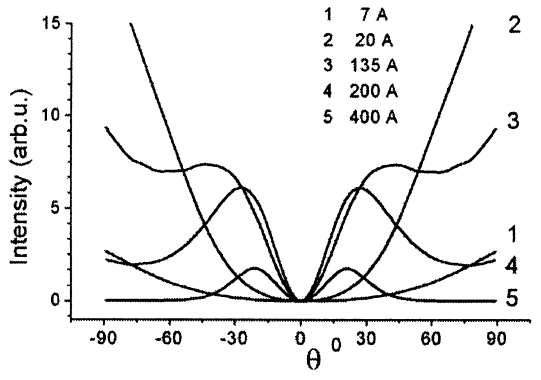

Figure 1 Size effect in DPE angular distributions. Intensity is plotted as a function of θ_2 at $\theta_1 = \phi_1 = \phi_2 = 0°$. Electron kinetic energies are $E_1 = 1\ eV$, $E_2 = 19\ eV$, emission occurs from the lowest level of the spherically symmetric oscillator of different sizes (radii shown nearby the curves).

a total wave-vector perpendicular to the field. The five curves 1-5 correspond to the quantum dot radii 7, 20, 135, 200 and 400 Å, respectively. If the dot is small enough (curves 1 and 2), the initial state is strongly localized. Roughly speaking, it's Fourier transform $\langle \mathbf{p}_3, \mathbf{k}_1 + \mathbf{k}_2 - \mathbf{p}_3 | \Phi_{12} \rangle$ is delocalized and smooth in a large domain of angles (θ_2, ϕ_2), therefore it adds no features to the angular distribution. This can be seen in Fig.2(a) which shows the three-dimensional plot of the case of curve 1, Fig.1. As $E_2 \gg E_1$, the sum $(\mathbf{k}_1 + \mathbf{k}_2)$ is almost parallel to vector $\mathbf{k}_2$. Since the PDE rate is proportional to $\hat{\epsilon}(\mathbf{k}_1 + \mathbf{k}_2)$ we notice a continuous increase of the curves 1,2 of Fig.1 towards $\theta_2 = \pm 90°$, where $\mathbf{k}_2$ becomes parallel to $\hat{\epsilon}$. The shape of Fig.2(a) can be understood from the following: as energy E_2 is much larger than E_1, the photon is "absorbed" mostly by the fast electron, which undergoes a dipole transition from the initially isotropic state, with a weak coupling to the second electron. This results in p-type distribution of the fast emitted photoelectron.

For larger sizes of the QDs the function $\langle \mathbf{p}_3, \mathbf{k}_1 + \mathbf{k}_2 - \mathbf{p}_3 | \Phi_{12} \rangle$ becomes rather localized at certain angles. One can think of this quantity

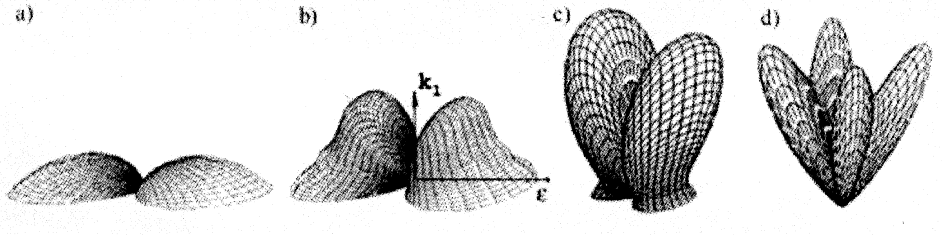

Figure 2 The same as Fig.1, 3D-view. Emission direction of the first electron and photon polarization direction are the same for all plots and are shown in plot (b). Radius of the well is (a) 7Å, (b) 135Å, (c) 200Å, (d) 400Å.

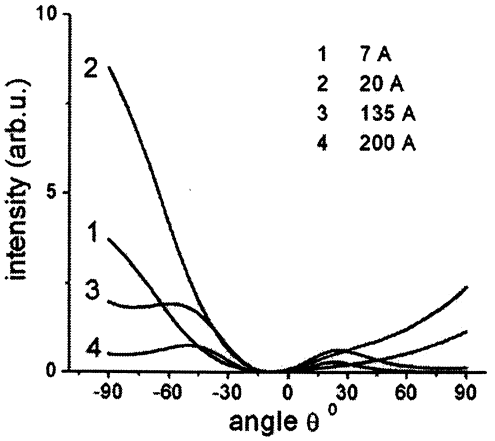

Figure 3 Conditions are the same as in Fig.1 except for the fixed dot size (7 Å) in z-direction and different angle $\theta_1 = 40°$. Lateral sizes are shown near the curves.

as of a measure of correlation in momentum space, probed by the vector $\mathbf{k}_1 + \mathbf{k}_2$. It affects the angular distribution by damping the certain (θ_2, φ_2)-regions as can be seen on the plots (b), (c), (d) (Fig.2), corresponding to curves 3, 4, 5 of Fig.1, respectively.

The second example demonstrates the effect of gradual broadening of a dot in lateral directions, keeping it's z-size equal to 7 Å. Four curves in Fig.3 correspond to xy-radii of 7, 20, 135 and 200 Å. To make geometry less symmetrical than in Fig.1, 1 eV electron is directed at 40 degrees from the normal to the xy-plane, the second electron has 19 eV kinetic energy. Again we observe the squeezing of the angular distributions, which is quite sensitive to the confinement in xy-plane. However, there is no continuous transition from a 3D-confinement (a dot) to 1D-confinement (a film) by taking a limit of infinite sizes of a dot in xy-directions. For very large lateral size DPE current from a dot goes to zero as soon as the overlap of the initial states in momentum space becomes vanishingly small. So, the case of a film must be considered independently.

4. ONE-DIMENSIONAL CONFINEMENT

Suppose the system is confined in z-direction and is infinite and jellium-like in x, y-directions. Accounting for the free motion parallel to the surface, irrespective of the other properties of the wave function, obtain:

$$\Phi_{p\|}(\mathbf{r}) = e^{i\mathbf{p}^{\|}\mathbf{r}^{\|}} \cdot \Phi^{\perp}(z), \qquad \left\langle \mathbf{q} \middle| \Phi_{p\|}(\mathbf{r}) \right\rangle = \delta(\mathbf{q}^{\|} - \mathbf{p}^{\|}) \cdot \left\langle q^{\perp} \middle| \Phi^{\perp} \right\rangle \quad (10)$$

$\mathbf{p}^{\|}$ is a component of the wave vector of the electron parallel to the surface, which is used as a quantum number denoting the state. Perpendicular component may be confined from two or one side so that to

represent a quantum well (modelled by square or parabolic well) or a layer on a surface (modelled by a triangular well). In both cases eigenstates of the potential in $\perp$-direction are the bottoms of two-dimensional single-particle subbands, filled by the motion in xy-directions. The energy conservation states the equality of initial and final state energies

$$E_i = -E_a^{\perp} - E_b^{\perp} + \frac{\mathbf{p}_a^{\parallel 2} + \mathbf{p}_b^{\parallel 2}}{2} + \hbar\omega_{ph} \quad \text{and} \quad E_f = \frac{k_1^2 + k_2^2}{2}. \tag{11}$$

Here and after all energies (relative to the vacuum) should be understood as absolute values and minus signs are written explicitly where necessary. $E_{a,b}^{\perp}$ are the eigenenergies of the a and b electrons in $\perp$-direction. The transition amplitude and cross section are:

$$\begin{aligned} T &\propto (\hat{\epsilon}\cdot\mathbf{K}^{+}) \int \mathrm{d}^3\mathbf{p}_3 \left\langle \frac{1}{2}(\mathbf{k}_2 - \mathbf{k}_1) \middle| \mathrm{G}_{12} \middle| \frac{1}{2}(\mathbf{k}_1 + \mathbf{k}_2) - \mathbf{p}_3 \right\rangle \times \\ &\times \langle \mathbf{p}_3, \mathbf{k}_1 + \mathbf{k}_2 - \mathbf{p}_3 | \Phi_{12} \rangle = \\ &= (\hat{\epsilon}\cdot\mathbf{K}^{+}) \int \mathrm{d}p_3^{\perp} \left\langle \frac{1}{2}(\mathbf{k}_2 - \mathbf{k}_1) \middle| \mathrm{G}_{12} \middle| \frac{1}{2}(\mathbf{k}_1 + \mathbf{k}_2) - \mathbf{p}_a^{\parallel} - p_3^{\perp} \right\rangle \times \\ &\times \left\langle p_3^{\perp}, k_1^{\perp} + k_2^{\perp} - p_3^{\perp} \middle| \Phi_{12}^{\perp} \right\rangle \delta(\mathbf{k}_1^{\parallel} + \mathbf{k}_2^{\parallel} - \mathbf{p}_a^{\parallel} - \mathbf{p}_b^{\parallel}) \end{aligned} \tag{12}$$

$$\frac{d\sigma}{dE_1 dE_2 d\Omega_1 d\Omega_2} \propto \int |T|^2 \, \delta\left(E_f - E_i\right) d^2\mathbf{p}_a^{\parallel} \mathrm{d}^2\mathbf{p}_b^{\parallel} \tag{13}$$

Conservation of the parallel component of the center of mass wave vector $\delta(\mathbf{k}_1^{\parallel} + \mathbf{k}_2^{\parallel} - \mathbf{p}_a^{\parallel} - \mathbf{p}_b^{\parallel})$ in Eq.(12) together with the conservation of energy from Eqs.(11),(13) eliminate integration over one of the vectors $\mathbf{p}_a^{\parallel}$ or $\mathbf{p}_b^{\parallel}$, and we are left with the two-dimensional integration over the initial state parallel component of one of the electrons. The z-component of the initial state is taken as a simple analytic one-parameter function, commonly used in the description of thin films, inversion layers, surface states, etc. [6; 7]:

$$\left|\Phi^{\perp}\right\rangle = \begin{cases} \sqrt{\frac{b^3}{2}} \cdot z \cdot \exp(-\frac{bz}{2}) & z > 0 \\ 0 & z < 0 \end{cases} \tag{14}$$

$$\left\langle q^{\perp} \middle| \Phi^{\perp} \right\rangle = \sqrt{\frac{b^3}{2}} \cdot \frac{1}{(iq^{\perp} + b/2)^2} \tag{15}$$

Two aspects will be demonstrated in the angular distributions: (i) the restrictions imposed by the energy and momentum conservation, and (ii)

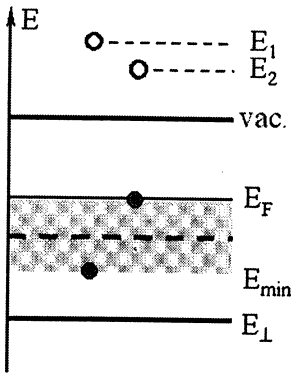

Figure 4 Energy diagram, showing kinetic energies E_1 and E_2, energy of the confinement in $\perp$-direction $E_\perp$ and integration range for $E_\parallel$ from the Fermi level to E_{min} (see text).

the role of screening. First one may be clarified by the energy diagram (Fig.4). Suppose for simplicity that both electrons have the same energy in z-direction $E = -E_\perp$ (all energies still given with respect to vacuum level with explicit minus signs). Due to the upper limit for the initial state energies (the Fermi energy $-E_F$), the integration region for $\mathbf{p}_a^{\parallel}$ in Eq.(13) also has an upper limit equal to $p_{max} = \sqrt{2(E_\perp - E_F)}$. So, parallel components of the initial state wave vectors should not leave the circle of the radius p_{max} in the xy-plane. At the same time, it has the lower limit, given by $p_{min} = \sqrt{2(E_F + E_\perp + E_1 + E_2 - \hbar\omega)} \geq 0$. Vectors $\mathbf{p}_a^{\parallel}, \mathbf{p}_a^{\parallel}$ are selected from within the ring of radii (p_{min}, p_{max}) so that to fulfill energy and momentum conservation. Note, that the longest possible $\mathbf{p}_a^{\parallel} + \mathbf{p}_b^{\parallel}$, that can be chosen from this ring, corresponds to the energy in the middle between E_F and E_{min} and equals to $p_{max}^{\parallel +} = 2\sqrt{E_1 + E_2 - \hbar\omega + 2E_\perp}$. This is the restriction, which prominently appears in the angular distributions by making certain final state geometries forbidden for DPE. For example, suppose for simplicity, that $\mathbf{k}_1$ is normal to xy-plane and fixed. This means that $\mathbf{p}_a^{\parallel} + \mathbf{p}_b^{\parallel} = \mathbf{k}_2^{\parallel}$. But such a condition may be not always fulfilled, if e.g. $\mathbf{k}_2^{\parallel}$ becomes long enough to exceed $p_{max}^{\parallel +}$. The similar considerations apply to less symmetrical geometries. This is demonstrated in Fig.5, where the vertical axis is the fixed θ_1-angle of the first electron, the horizontal axis is the variable θ_2-angle of the second electron, and the hatched region between two curves gives the allowed values of θ_2 for the given θ_1 (θ_2 varies in plane $\varphi = 0$). For the case of equal kinetic energies of two electrons the zero in the angular distribution due to the selection rule will be always present (diagonal line fully inside the hatched region), and the zero due to the Coulomb repulsion will be visible only at some angles θ_1 (second diagonal). Sharp cut-off of angular distributions may serve as

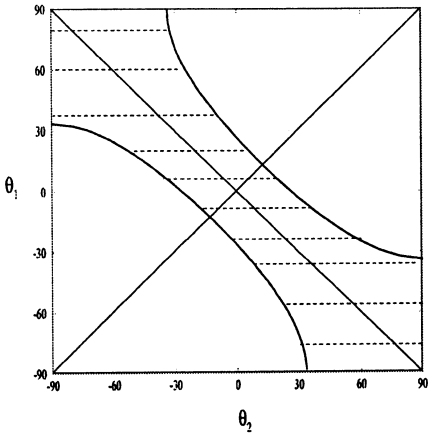

Figure 5 Example of the angular restrictions imposed by the energy and momentum conservation. At a given θ_1 the value of θ_2 inside the hatched region is only possible. Two diagonal lines show the positions of zeros of angular distribution due to the selection rule and Coulomb repulsion, electron kinetic energies are equal.

an additional information for the estimation of bound state energies in $\perp$-direction with respect to the Fermi level.

The remaining electrons screen the mutual Coulomb interaction within the ejected electron pair. The simplest model to account for this shielding effect is given by the Thomas-Fermi theory which derives the electron-electron potential as

$$U(r_{12}) = \frac{\exp(-\lambda r_{12})}{r_{12}}, \qquad U_q = \frac{4\pi}{q^2 + \lambda^2}. \tag{16}$$

The momentum-space potential U_q indicates the decay rate of the two-body interaction as a function of the inverse screening length λ, which is in turn determined by the mean electronic density. It is not possible to proceed in the non-perturbative way as we did for the bare Coulomb interaction because there is no closed-form expression for the Green function of the screened interaction. Continuum wave function of the screened Coulomb potential does not have well-defined zero-screening limit [5]. Therefore we adhere to a perturbative framework.

The first-order Green's function in screened Coulomb interaction $G_{12} \approx G_0 U G_0$ is the first finite term in perturbation series of G_{12} (the zero-order term $G_{12} \approx G_0$ reduces the problem to the single-particle one and T vanishes). The 6-fold DPE cross section reads

$$\begin{aligned} \frac{d\sigma}{dE_1 dE_2 d\Omega_1 d\Omega_2} &\propto \int \delta(E_i - E_f)\delta(\mathbf{k}_1^{\parallel} + \mathbf{k}_2^{\parallel} - \mathbf{p}_a^{\parallel} - \mathbf{p}_b^{\parallel}) \mathrm{d}^3\mathbf{p}_a \mathrm{d}^3\mathbf{p}_b \times \\ \times & \left| (\hat{\epsilon} \cdot \mathbf{K}^+) \int \mathrm{dp}^{\perp} \left\langle \frac{1}{2}(\mathbf{k}_2 - \mathbf{k}_1) \middle| \mathrm{G_0 U G_0} \middle| \frac{1}{2}(\mathbf{k}_1 + \mathbf{k}_2) - \mathrm{p}^{\perp} - \mathbf{p}_a^{\parallel} \right\rangle \right|^2 \\ \times & \left| \left\langle p^{\perp}, k_1^{\perp} + k_2^{\perp} - p^{\perp} \middle| \Phi_{12}^{\perp} \right\rangle \right|^2 . \end{aligned} \tag{17}$$

Note that the unscreened Coulomb potential favors small momentum transfer, i.e. large-distance, interactions. This situation changes when the interaction is shielded. In the extreme of very strong shielding $\lambda \gg 1$ only very large momentum transfers $q \geq \lambda$ (hard collisions) do contribute to T. The possible geometry to visualize the role of screening is shown in Fig.6(b). Both electrons have equal energies and equal angles with respect to the surface normal. The polarization vector is normal to the surface and parallel to $\mathbf{k}_1 + \mathbf{k}_2$. Let's increase both angles θ_1, θ_2 gradually and simultaneously from 0 to 90^0, so that $\mathbf{k}_1 + \mathbf{k}_2$ remains always perpendicular to the surface. Fig.6(a) shows the DPE cross section as a function of θ=θ_1=θ_2. Two curves correspond to two values of λ. We remark at first that the intensity, in particular at the maximum, falls down with increasing λ. This is shown explicitly in Fig.6(c) and is evident from the fact that the DPE process depends on the strength of interaction between the electrons. Furthermore we notice that the angular position of maximum in Fig.6(a) grows with increasing λ (Fig.6(b)). I.e. for more effective screening the photoelectrons escape at larger mutual angles. At $\theta_1 = 0$ no emission happens because electrons can not

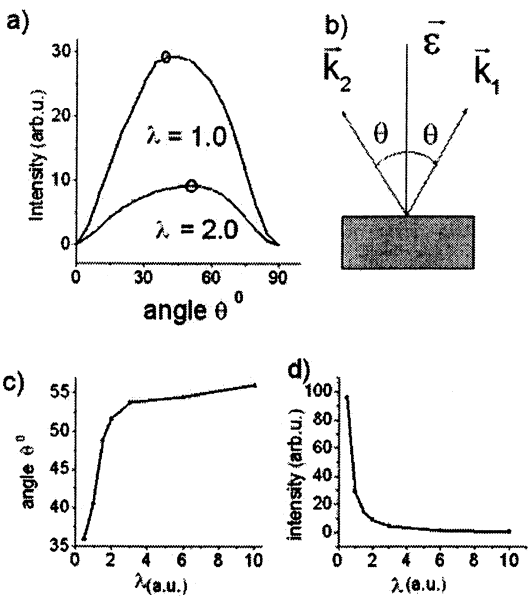

Figure 6 Dependence of the DPE angular distributions on screening: (a) angular distributions at two values of λ, circles show the maxima; (b) sketch of the experimental geometry: $\varphi_1 = \varphi_2 = 0$, $\theta_1 = \theta_2 = \theta$ from 0° to 90°;(c) position of the maximum as a function of λ; (d) DPE intensity in the maximum as a function of λ.

follow the same direction with the same energies. At $\theta_1 = 90$ emission is impossible because of the DPE selection rules. The maximum is somewhere in between and finally seems to saturate with λ. Noteworthy, that the shift of the maximum with changing λ is purely due to the dynamics (changes in the matrix element) of DPE. So, within the static screening concept the material-dependent parameter λ can be related to the maxima in angular distributions, and hence the most efficient experimental conditions can be estimated. For example, for the values of inverse screening length between 1 and 2 a.u. (holds for quite a lot of metals) the favorable observation condition would be to set the angle of about 80°-90° between the detectors.

5. CONCLUSION

The focus of this work has been put on the manifestation of quantum size and correlation effects in DPE spectra for the systems with different degree of confinement. We discussed simple systems, a quantum dot and a thin film, and found out three main features in the DPE angular distributions, which could be attributed to the confinement effects. First, the size of a quantum dot can effect the appearance of the angular correlation plots substantially, and this is related to the degree of localization of quantum dot bound states. Second, the energetics of the film band structure can impose prominent restrictions on the allowed ejection geometry. Third, the influence of screening on the DPE angular distributions was investigated. It was found that the positions of their maxima are sensitive to the value of the screening length, and this is a matter of further investigation whether it is an effect due to the first-order approximation or it is a general conclusion.

References

[1] R. Herrmann, S. Samarin, H. Schwabe, and J. Kirschner Phys.Rev.Lett. 81, 2148 (1998)
[2] J. Berakdar, Phys.Rev.B 58, 9808 (1998)
[3] N. Fominykh, J. Henk, J. Berakdar, P. Bruno, H. Gollisch, R. Feder, Sol.State Commun. 113, 665 (2000)
[4] M. Rontani, F. Rossi, F. Manghi, E. Molinari, Phys. Rev. B, 59, 10165 (1999)
[5] J. Chen, A. Chen Adv. At. Mol. Phys. 17, 71 (1972)
[6] T. Ando, A. Fowler, F. Stern, Rev. Mod. Phys. 54, 437 (1982)
[7] P. Harrison, Quantum Wells, Wires and Dots, John Wiley, UK, 2000.